

Research Article

Dipolariton Formation in Quantum Dot Molecules Strongly Coupled to Optical Resonators

Marlon S. Domínguez, David F. Macias-Pinilla , and Hanz Y. Ramírez 

Grupo de Física Teórica y Computacional, Escuela de Física, Universidad Pedagógica y Tecnológica de Colombia (UPTC), Tunja, 150003 Boyacá, Colombia

Correspondence should be addressed to Hanz Y. Ramírez; hantz.ramirez@uptc.edu.co

Received 31 July 2018; Revised 16 October 2018; Accepted 7 November 2018; Published 31 January 2019

Guest Editor: Abdoulaye Ndao

Copyright © 2019 Marlon S. Domínguez et al. This is an open access article distributed under the Creative Commons Attribution License, which permits unrestricted use, distribution, and reproduction in any medium, provided the original work is properly cited.

In this theoretical work, we study a double quantum dot interacting strongly with a microcavity, while undergoing resonant tunneling. Effects of interdot tunneling on the light-matter hybridized states are determined, and tunability of their brightness degrees, associated dipole moments, and lifetimes is demonstrated. These results predict dipolariton generation in artificial molecules coupled to optical resonators and provide a promising scenario for the control of emission efficiency and coherence times of exciton polaritons.

1. Introduction

In recent years, interest for light generation from low-dimensional structures coupled to electrodynamics cavities has increased noticeably [1–3]. In particular, quantum dots (QDs) have proved to be an excellent tool for experimental observation of purely quantum phenomena, like single-photon emission and photon entanglement, both of which can be enhanced through an optical resonator by strengthening the coupling between the QD and the electromagnetic field [4–6].

Those high-quality nanostructured semiconductors that can be obtained by molecular beam epitaxy (MBE) or chemical vapor deposition (CVD) [7] have exhibited relevant atom-like phenomena such as Rabi oscillations [8, 9], Mollow triplet in resonance fluorescence [10, 11], Dicke effect [12, 13], and double dressing resonances [14, 15]. Consequently, they are often called “artificial atoms.”

Considering the implementation of electronic devices, the use of artificial atoms instead of natural ones would be advantageous, given the obvious convenience of working with stable solid structures rather than with tiny and elusive atoms, for constructing on-chip light-matter hybrid structures [16].

In turn, microcavities confine light in a small volume and increase radiation-matter coupling as described by the Purcell effect [17, 18]. In such a strong coupling regime, the system eigenvectors are hybridized states of the QD and the cavity field. These kinds of mixed states of light and matter are known as “exciton polaritons” (EPs) [19, 20]. Strong radiation-matter coupling for a QD inside either planar or photonic crystal cavities has been successfully observed and progressively improved along this century, including electron spin states in charged excitons [10, 18, 21, 22].

On the other hand, coupling by resonant tunneling between adjacent QDs (artificial molecules) has been proposed as an efficient mechanism to improve tunability in zero-dimensional systems [23, 24]. Between different alternatives to control tunneling in double-quantum dot (DQD) structures, bias tuning has been found so far as the most successful [25–27].

For instance, recent experiments have taken advantage of interdot coupling in artificial molecules within QED cavities, for the enhancement of hybrid qubits [28], for the manipulation of light-matter interaction with superconducting resonators [29], for the improvement of single-photon emission [30], and for the observation of phonon-assisted cavity feeding [31].

Regarding two-dimensional systems, several theoretical and experimental efforts have been carried out toward controllable condensation of multiexciton states in double-quantum wells inside cavities [32–37]. Those works revealed the characteristic three branches associated to tunnel-coupled structures, which in the 2D case correspond to polariton bands instead of fully discretized polariton states [38, 39]. In contrast, reports on dipolaritons in 0D systems are scarce, despite of their potential usefulness as the sources of nonclassical light and quantum memories [40].

As for the direct measurement of coherent superpositions of light-matter states in QD-cavity systems, it has been achieved by a few recent experiments [3, 19, 41, 42], in all cases using individual dots.

In this work, we study the properties at the small photon number scale of EP modes for a DQD embedded in a microcavity, in such a way that interdot coupling and strong radiation-matter interaction are simultaneously considered and formation of polaritons with adjustable dipole moment (dipolaritons) and reduced brightness (dark polaritons) is explored [32]. Hopefully, this investigation may contribute with deeper understanding toward the imminent experimental realization of light-matter hybridized states in DQD-based settings.

2. Model

We consider an asymmetric double quantum dot with a slight difference in the intrinsic energy of the direct and indirect excitonic levels, coupled to a microcavity. Figure 1(a) depicts the proposed system, in which J represents the coupling between the left and right dots (LD-RD), while Figure 1(b) shows the configurations chosen as the basis of the subspace corresponding to the first rung of the Jaynes-Cummings (JC) ladder [43].

In the absence of a bias field, the direct exciton (DX) coupled to a photonic mode would form a conventional polariton with a coupling energy given by the Rabi frequency Ω (which in turn depends on the radiation-matter constant g) [15]. On its side, the indirect exciton (IX) is assumed to be a dark state, given the reduced overlap between the electron and hole.

Application of an external bias F on the DQD allows for tuning of the indirect exciton energy, so that resonant tunneling between the $|0, DX\rangle$ and $|0, IX\rangle$ states can be achieved on-demand.

The tunneling rate J depends on the potential barrier experienced by the confined single particles and is in principle unmodified by the cavity. For simplicity, hole tunneling can be reasonably neglected, and then, only electron hopping is considered [27].

The Hamiltonian for the n -th JC rung in the above described basis reads ($\hbar = 1$)

$$\begin{aligned} \hat{H} = & \omega_C \hat{n} - \Delta_{c,dx} \hat{\sigma}_{dx,g}^\dagger \hat{\sigma}_{g,dx}^- + (\Delta_{ix,dx} - \Delta_{c,dx} - edF) \hat{\sigma}_{ix,g}^\dagger \hat{\sigma}_{g,ix}^- \\ & + g \left(\hat{a} \hat{\sigma}_{dx,g}^\dagger + \hat{a}^\dagger \hat{\sigma}_{g,dx}^- \right) - \frac{J}{2} \left(\hat{\sigma}_{dx,g}^\dagger \hat{\sigma}_{g,ix}^- + \hat{\sigma}_{ix,g}^\dagger \hat{\sigma}_{g,dx}^- \right), \end{aligned} \quad (1)$$

where ω_C is the cavity mode frequency, e is the electron charge, d is the interdot distance (tunneling barrier width), $\Delta_{ix,dx} = \omega_{IX} - \omega_{DX}$ ($\Delta_{c,dx} = \omega_C - \omega_{DX}$) is the energy difference between the IX and DX (the cavity mode and the DX), $\hat{n} = \hat{a}^\dagger \hat{a} + \hat{\sigma}_{dx,g}^\dagger \hat{\sigma}_{g,dx}^- + \hat{\sigma}_{ix,g}^\dagger \hat{\sigma}_{g,ix}^-$ is the polariton number operator (with \hat{a} and \hat{a}^\dagger as the photon annihilation and creation operators, respectively), and $\hat{\sigma}_{dx,g}^\dagger = |DX\rangle\langle g|$ ($\hat{\sigma}_{ix,g}^\dagger = |IX\rangle\langle g|$) is the transition dipole operator between the DX (IX) and the DQD ground state.

The control parameter is the electric field F , which allows compensating $\Delta_{ix,dx}$ to favor resonant tunneling between dots. Tuning by electrical means is chosen, because as mentioned in the introduction, electric fields have successfully been used as a control mechanism in structures coupled by tunneling [26].

Whether the cavity is a photonic crystal, a micropillar, or an arrangement of Bragg mirrors is irrelevant for the model. What becomes important is the existence of a well-defined electromagnetic mode, whose energy difference with the ground direct and indirect excitons can be much smaller than the difference between cavity eigenfrequencies. This allows neglecting not just other modes in the cavity but also the excited levels in each dot constituting the artificial molecule (supposing dots at the order of the few nanometers in height and radius as the ones used in the current quantum optical experiments).

To obtain the bias-dependent radiative lifetimes of the EP eigenstates and their corresponding decay rates, which determine the dynamics of the system at a very-low temperature, where phonon dissipation effects can be ignored, we use the imaginary part of the effective Hamiltonian yielded by equation (1).

$$\hat{H}_{\text{eff}} \begin{pmatrix} \omega_c n + \Delta_{IX,DX} - \Delta_{c,DX} - edF & -\frac{J}{2} & 0 \\ -\frac{i}{2}(n-1)\kappa & \omega_c n - \Delta_{c,DX} - \frac{i}{2}\gamma_{DX} & \\ -\frac{J}{2} & -\frac{i}{2}(n-1)\kappa & \frac{\Omega_R}{2} = g\sqrt{n} \\ 0 & \frac{\Omega_R}{2} = g\sqrt{n} & \omega_c n - \frac{i}{2}n\kappa \end{pmatrix}, \quad (2)$$

in which κ represents the cavity scape rate of photons and γ_{DX} is the direct exciton recombination rate (we neglect the indirect exciton recombination because of the poor electron-hole overlap in this configuration, i.e., $\gamma_{DX} = 0$).

Thus, the real and imaginary parts of the eigenvalues of the matrix in equation (2), respectively, provide the EP energies and coherence times of the artificial molecule-cavity system, as functions of the externally applied electric field.

3. Results

By diagonalizing the Hamiltonian in equation (1), the EP modes and their corresponding energies can be obtained ($|1, \text{UP}\rangle$, $|1, \text{MP}\rangle$, and $|1, \text{LP}\rangle$). Figure 2(a) shows the uncoupled and EP energies for the first JC rung as functions

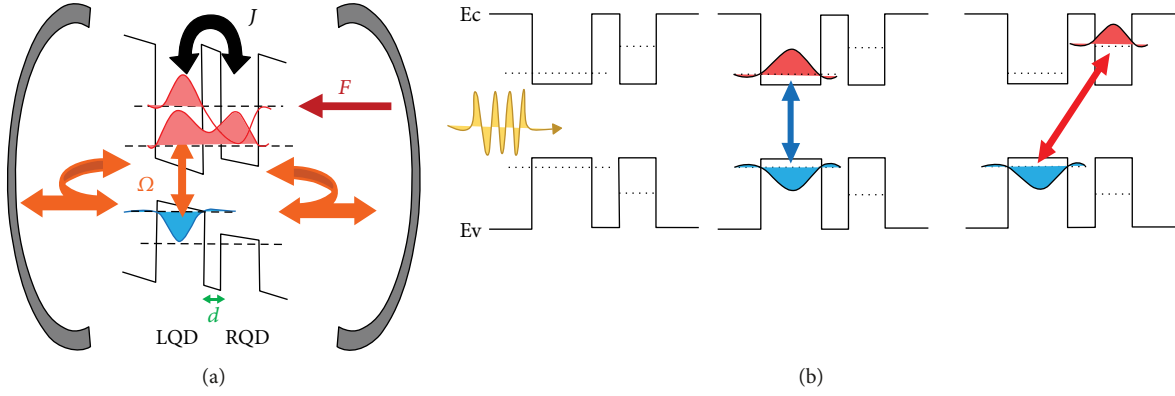
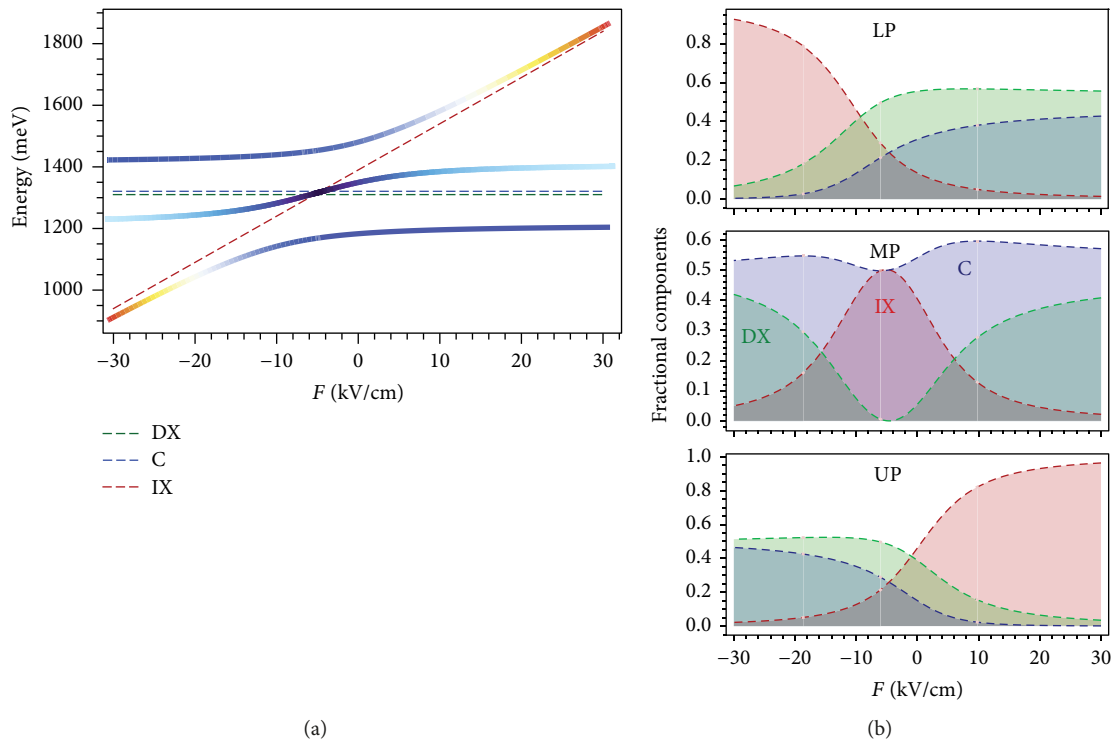


FIGURE 1: (a) Schematics of the studied system. (b) Configuration basis.

FIGURE 2: (a) Lower, middle, and upper polariton modes as functions of the bias field F . (b) Fractional bare components for each of the polariton modes, as functions of F .

of the bias field F . Dashed lines describe uncoupled modes (IX: red, C: blue, and DX: green), and the solid lines blue and light blue represent the polariton and dipolariton, respectively. Meanwhile, Figure 2(b) shows the fractional components of the basis states (Hopfield coefficients), for each of the EP modes. The following realistic parameters were used in our calculations: $\omega_c = 1320.7$ meV, $\Delta_{ix,dx} = 80$ meV, $\Delta_{c,dx} = 10.7$ meV, $d = 15$ nm, $J = 0.828$ meV, $g = 2\pi 16$ GHz, and $\Omega = J$. Under such conditions, the tunneling resonance is found at -5.75 kV/cm. This is a remarkably moderate field, very accessible in experiments, in contrast to the high fields necessary for dipolariton manipulation achieved by magnetic means (larger than 5 teslas), as found by Rojas-Arias et al. [40].

From the obtained coefficients shown in Figure 2(b), two associated quantities can be computed to better elucidate the enriched polariton landscape produced by the presence of the second dot. Denoting the EP modes by $|1, LP\rangle$, $|1, MP\rangle$, and $|1, UP\rangle$ and considering the superposition,

$$|1, \alpha\rangle = C_{1,g}^\alpha |1, g\rangle + C_{0,DX}^\alpha |0, DX\rangle + C_{0,IX}^\alpha |0, IX\rangle, \quad (3)$$

where $\alpha = LP, MP, \text{ and } UP$; for each EP mode α , we define the bright polariton degree

$$\text{BPD} = \left| C_{1,g}^\alpha C_{0,DX}^\alpha \right| \quad (4)$$

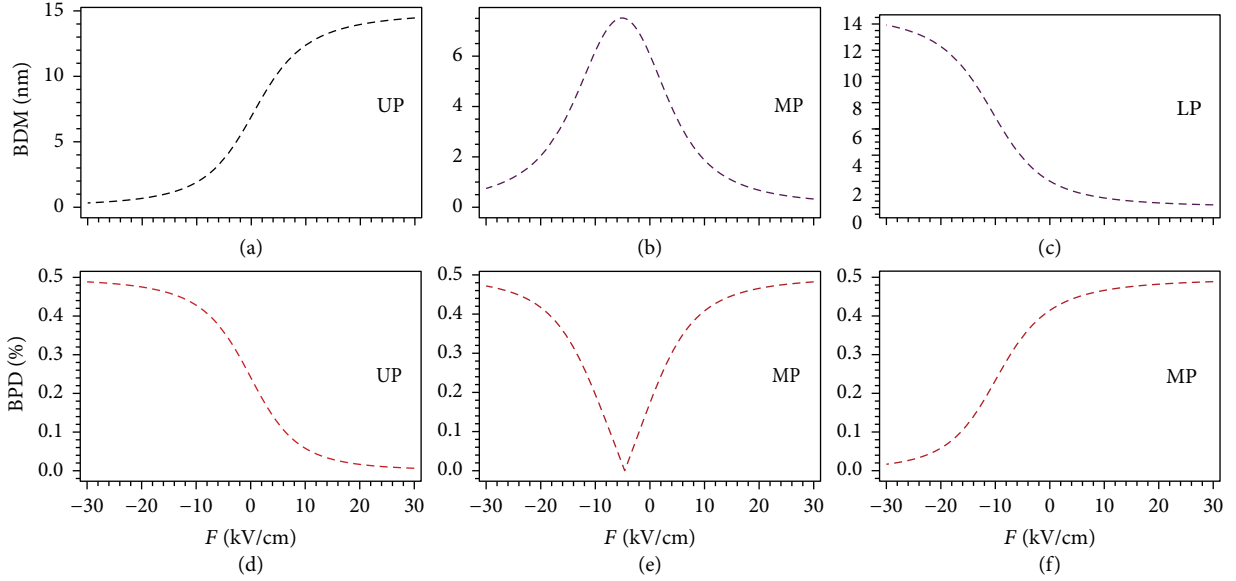


FIGURE 3: Exciton dipole moments for the (a) upper, (b) middle, and (c) lower polariton modes. Bright polariton degree for the (d) upper, (e) middle, and (f) lower polariton modes. Both quantities as functions of F .

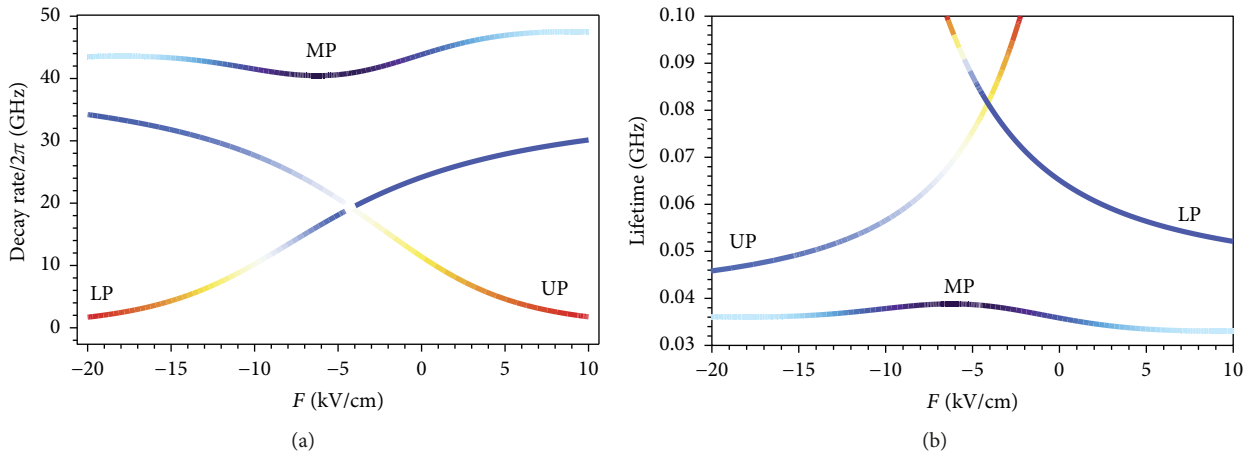


FIGURE 4: (a) Polariton decay rate and (b) polariton lifetime for each EP mode, as functions of F .

and the exciton dipole moment

$$\text{EDM} = d |C_{0,IX}^\alpha|. \quad (5)$$

BPD indicates how strong is the mixing between the DX and the cavity mode, and EDM accounts for the dipole moment associated to the corresponding EP mode.

Figure 3 shows the BPD and EDM as functions of the bias field F , for the same parameters as in Figure 2. There, three regimes generated by the interplay between light-matter and interdot coupling, can be observed: (I) conventional polariton [bright radiation-matter-mixed states with negligible exciton dipole moment], for negative (positive) high values of F in the upper (lower) EP mode and for positive and negative high values of in the middle EP mode; (II) dark dipolariton [mixed radiation matter states with negligible brightness and large dipole moment], for

values of F just around the tunneling resonance, in the middle EP mode; and (III) bright dipolariton [mixed radiation matter states with significant brightness and exciton dipole moment], for moderate values of F (as long as they are not very close to the tunneling resonance), in the middle EP mode.

Regimes (II) and (III) are particularly interesting: the former because this type of polariton states are expected to be long-living bosons, promising for exciton condensates and derived applications [44], and the later, because a tunable mixing between bright conventional polaritons and dark dipolaritons provides an optimal scenario for on-demand switching between their respective main features.

The effective tunability by electrical means of the polariton dipole moment (across one order of magnitude), shown in Figures 3(a)–3(c), is particularly suggesting and has been not reported in previous related works.

To evidence how polariton lifetimes can be tuned along a wide range, we calculate the system dynamics by diagonalizing

the complex matrix of equation (2) [19]. Figure 4 shows the bias field dependence of the recombination rates and lifetimes of all three polaronic branches. The parameters $\gamma_{DX} = 2\pi \cdot 0.1$ GHz and $\kappa = 2\pi \cdot 16$ GHz were used in the simulation.

Those curves reveal how the lower and upper branches allow tuning the polariton lifetimes between tens and hundreds of picoseconds, by the application of modest bias (below $|F| < 20$ kV/cm). Furthermore, comparing these lifetimes with the ones reported in Figures 2(b) and 2(d) of reference [3], one can appreciate how their modulation along similar time ranges requires significant temperature fluctuations, which unavoidably imply phonon-related dissipation and dephasing. This evidences improved coherence and stability associated to electric control.

4. Conclusion

In this work, we presented a theoretical model for a quantum dot molecule strongly coupled to a microcavity, which allows the calculation of the composed system eigenenergies, as well as of the corresponding eigenstates (dressed states) and radiative decay rates. From the simulated fractional components and polariton lifetimes, as functions of a feasible tuning parameter (electric field), the possibility of generating polaritons with enhanced exciton dipole moment and adjustable emission efficiency and duration is demonstrated.

These results suggest that the proposed combination of artificial molecules with optical resonators could foster improved control of coherence times and on-demand emission of nonclassical light from strongly coupled light-matter arrangements. Thus, further motivation for the experimental realization of exciton polaritons from double-quantum dot-cavity settings is provided.

Data Availability

Supporting data would be available on reasonable request.

Conflicts of Interest

The authors declare they have no conflict of interest.

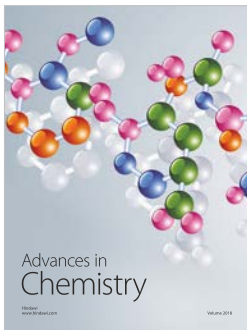
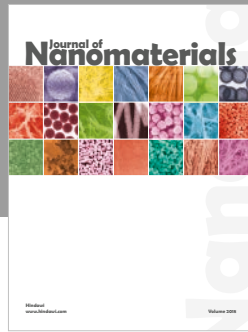
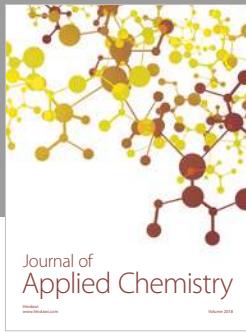
Acknowledgments

Financial support from the research division of the Universidad Pedagógica y Tecnológica de Colombia (UPTC), under grant SGI-2527, is acknowledged.

References

- [1] A. Kubanek, A. Ourjoumtsev, I. Schuster et al., “Two-photon gateway in one-atom cavity quantum electrodynamics,” *Physical Review Letters*, vol. 101, no. 20, article 203602, 2008.
- [2] K. Hennessy, A. Badolato, M. Winger et al., “Quantum nature of a strongly coupled single quantum dot–cavity system,” *Nature Physics*, vol. 445, no. 7130, pp. 896–899, 2007.
- [3] K. Müller, K. A. Fischer, A. Rundquist et al., “Ultrafast polariton-phonon dynamics of strongly coupled quantum dot-nanocavity systems,” *Physical Review X*, vol. 5, no. 3, article 031006, 2015.
- [4] F. Hargart, M. Mller, K. Roy-Choudhury et al., “Cavity-enhanced simultaneous dressing of quantum dot exciton and biexciton states,” *Physical Review B*, vol. 93, no. 11, article 115308, 2016.
- [5] D. Xing, H. Yu, Z. C. Duan et al., “On-demand single photons with high extraction efficiency and near-unity indistinguishability from a resonantly driven quantum dot in a micropillar,” *Physical Review Letters*, vol. 116, no. 2, 2016.
- [6] O. J. Gómez-Sánchez and H. Y. Ramírez, “Solid-state emitter embedded in a microcavity under intense excitation: A variational master-equation approach,” *Physical Review A*, vol. 98, no. 5, article 053846, 2018.
- [7] E. Borovitskaya and M. S. Shur, *Quantum Dots*, Vol. 25, World Scientific, 2002.
- [8] H. Y. Ramírez and A. S. Camacho, “Coupling effects on Rabi oscillations in quantum dots chains,” *Physica E: Low-dimensional Systems and Nanostructures*, vol. 40, no. 9, pp. 2937–2940, 2008.
- [9] E. B. Flagg, A. Muller, J. W. Robertson et al., “Resonantly driven coherent oscillations in a solid-state quantum emitter,” *Nature Physics*, vol. 5, no. 3, pp. 203–207, 2009.
- [10] A. N. Vamivakas, Y. Zhao, C.-Y. Lu, and M. Atatüre, “Spin-resolved quantum-dot resonance fluorescence,” *Nature Physics*, vol. 5, no. 3, pp. 198–202, 2009.
- [11] A. Ulhaq, S. Weiler, S. M. Ulrich, R. Roßbach, M. Jetter, and P. Michler, “Cascaded single-photon emission from the Mollow triplet sidebands of a quantum dot,” *Nature Photonics*, vol. 6, no. 4, pp. 238–242, 2012.
- [12] T. Vorrath and T. Brandes, “Dicke effect in the tunnel current through two double quantum dots,” *Physical Review B*, vol. 68, no. 3, article 035309, 2003.
- [13] P. A. Orellana, G. A. Lara, and A. E. V., “Kondo and Dicke effect in quantum dots side coupled to a quantum wire,” *Physical Review B*, vol. 74, no. 19, article 193315, 2006.
- [14] H. Y. Ramírez, “Double dressing and manipulation of the photonic density of states in nanostructured qubits,” *RSC Advances*, vol. 3, no. 47, article 24991, 2013.
- [15] Y. He, Y. M. He, J. Liu et al., “Dynamically controlled resonance fluorescence spectra from a doubly dressed single InGaAs quantum dot,” *Physical Review Letters*, vol. 114, no. 9, article 097402, 2015.
- [16] I. Aharonovich, D. Englund, and M. Toth, “Solid-state single-photon emitters,” *Nature Photonics*, vol. 10, no. 10, pp. 631–641, 2016.
- [17] E. M. Purcell, H. C. Torrey, and R. V. Pound, “Resonance absorption by nuclear magnetic moments in a solid,” *Physical Review*, vol. 69, no. 1-2, pp. 37–38, 1946.
- [18] P. Lodahl, S. Mahmoodian, and S. Stobbe, “Interfacing single photons and single quantum dots with photonic nanostructures,” *Reviews of Modern Physics*, vol. 87, no. 2, pp. 347–400, 2015.
- [19] K. Müller, A. Rundquist, K. A. Fischer et al., “Coherent generation of nonclassical light on chip via detuned photon blockade,” *Physical Review Letters*, vol. 114, no. 23, 2015.
- [20] C. Schneider, K. Winkler, M. D. Fraser et al., “Exciton-polariton trapping and potential landscape engineering,” *Reports on Progress in Physics*, vol. 80, no. 1, article 016503, 2017.
- [21] Y. M. He, Y. He, Y. J. Wei et al., “On-demand semiconductor single-photon source with near-unity indistinguishability,” *Nature Nanotechnology*, vol. 8, no. 3, pp. 213–217, 2013.

- [22] S. G. Carter, T. M. Sweeney, M. J. Kim et al., “Quantum control of a spin qubit coupled to a photonic crystal cavity,” *Nature Photonics*, vol. 7, no. 4, pp. 329–334, 2013.
- [23] H. Y. Ramírez, A. S. Camacho, and L. C. L. Y. Voon, “Influence of shape and electric field on electron relaxation and coherent response in quantum-dot molecules,” *Journal of Physics: Condensed Matter*, vol. 19, no. 34, article 346216, 2007.
- [24] N. R. Fino, A. S. Camacho, and H. Y. Ramírez, “Coupling effects on photoluminescence of exciton states in asymmetric quantum dot molecules,” *Nanoscale Research Letters*, vol. 9, no. 1, p. 297, 2014.
- [25] H. Y. Ramírez, A. S. Camacho, and L. C. Lew Yan Voon, “DC electric field effects on the electron dynamics in double rectangular quantum dots,” *Brazilian Journal of Physics*, vol. 36, no. 3b, pp. 869–873, 2006.
- [26] E. A. Stinaff, M. Scheibner, A. S. Bracker et al., “Optical signatures of coupled quantum dots,” *Science*, vol. 311, no. 5761, pp. 636–639, 2006.
- [27] A. S. Bracker, M. Scheibner, M. F. Doty et al., “Engineering electron and hole tunneling with asymmetric InAs quantum dot molecules,” *Applied Physics Letters*, vol. 89, no. 23, p. 233110, 2006.
- [28] P. M. Vora, A. S. Bracker, S. G. Carter et al., “Spin–cavity interactions between a quantum dot molecule and a photonic crystal cavity,” *Nature Communications*, vol. 6, no. 1, article 7665, 2015.
- [29] A. Stockklauser, P. Scarlino, J. V. Koski et al., “Strong coupling cavity QED with gate-defined double quantum dots enabled by a high impedance resonator,” *Physical Review X*, vol. 7, no. 1, article 011030, 2017.
- [30] D. Gammon, S. Carter, A. S. Bracker, and P. Vora, “Single photon source based on a quantum dot molecule in an optical cavity,” US Patent US9619754B2, 2017.
- [31] T. R. Hartke, Y. Y. Liu, M. J. Gullans, and P. J. R., “Microwave detection of electron-phonon interactions in a cavity-coupled double quantum dot,” *Physical Review Letters*, vol. 120, no. 9, article 097701, 2018.
- [32] P. Cristofolini, G. Christmann, S. I. Tsintzos et al., “Coupling quantum tunneling with cavity photons,” *Science*, vol. 336, no. 6082, pp. 704–707, 2012.
- [33] J. Y. Li, S. Q. Duan, and W. Zhang, “ac-field-modulated terahertz radiation based on dipolaritons,” *Europhysics Letters*, vol. 108, no. 6, article 67010, 2014.
- [34] T. Byrnes, G. V. Kolmakov, R. Y. Kezerashvili, and Y. Yamamoto, “Effective interaction and condensation of dipolaritons in coupled quantum wells,” *Physical Review B*, vol. 90, no. 12, article 125314, 2014.
- [35] K. Sivalertporn and E. A. Muljarov, “Controlled strong coupling and absence of dark polaritons in microcavities with double quantum wells,” *Physical Review Letters*, vol. 115, no. 7, article 077401, 2015.
- [36] I. Rosenberg, Y. Mazuz-Harpaz, R. Rapaport, K. West, and L. Pfeiffer, “Electrically controlled mutual interactions of flying waveguide dipolaritons,” *Physical Review B*, vol. 93, no. 19, article 195151, 2016.
- [37] E. Togan, H. T. Lim, S. Faelt, W. Wegscheider, and A. Imamoglu, “Strong interactions between dipolar polaritons,” 2018, <http://arxiv.org/abs/1804.04975>.
- [38] J. Wilkes and E. A. Muljarov, “Excitons and polaritons in planar heterostructures in external electric and magnetic fields: a multi-sub-level approach,” *Superlattices and Microstructures*, vol. 108, pp. 32–41, 2017.
- [39] P. I. Khadzhi, O. F. Vasilieva, and I. V. Belousov, “Dynamics of a dipolariton optical parametric oscillator in a semiconductor microcavity,” *Journal of Experimental and Theoretical Physics*, vol. 126, no. 2, pp. 147–158, 2018.
- [40] J. S. Rojas-Arias, B. A. Rodriguez, and H. Vinck-Posada, “Magnetic control of dipolaritons in quantum dots,” *Journal of Physics: Condensed Matter*, vol. 28, no. 50, article 505302, 2016.
- [41] C. Dory, K. A. Fischer, K. Müller et al., “Complete coherent control of a quantum dot strongly coupled to a nanocavity,” *Scientific Reports*, vol. 6, no. 1, article 25172, 2016.
- [42] N. Y. Jia, N. Schine, A. Georgakopoulos et al., “A strongly interacting polaritonic quantum dot,” *Nature Physics*, vol. 14, no. 6, pp. 550–554, 2018.
- [43] J. Cotrino-Lemus and H. Y. Ramírez, “Efficiently tunable photon emission from an optically driven artificial molecule,” *Journal of Physics: Conference Series*, vol. 864, article 012081, 2017.
- [44] T. Byrnes, N. Y. Kim, and Y. Yamamoto, “Exciton–polariton condensates,” *Nature Physics*, vol. 10, no. 11, pp. 803–813, 2014.



Hindawi

Submit your manuscripts at
www.hindawi.com

